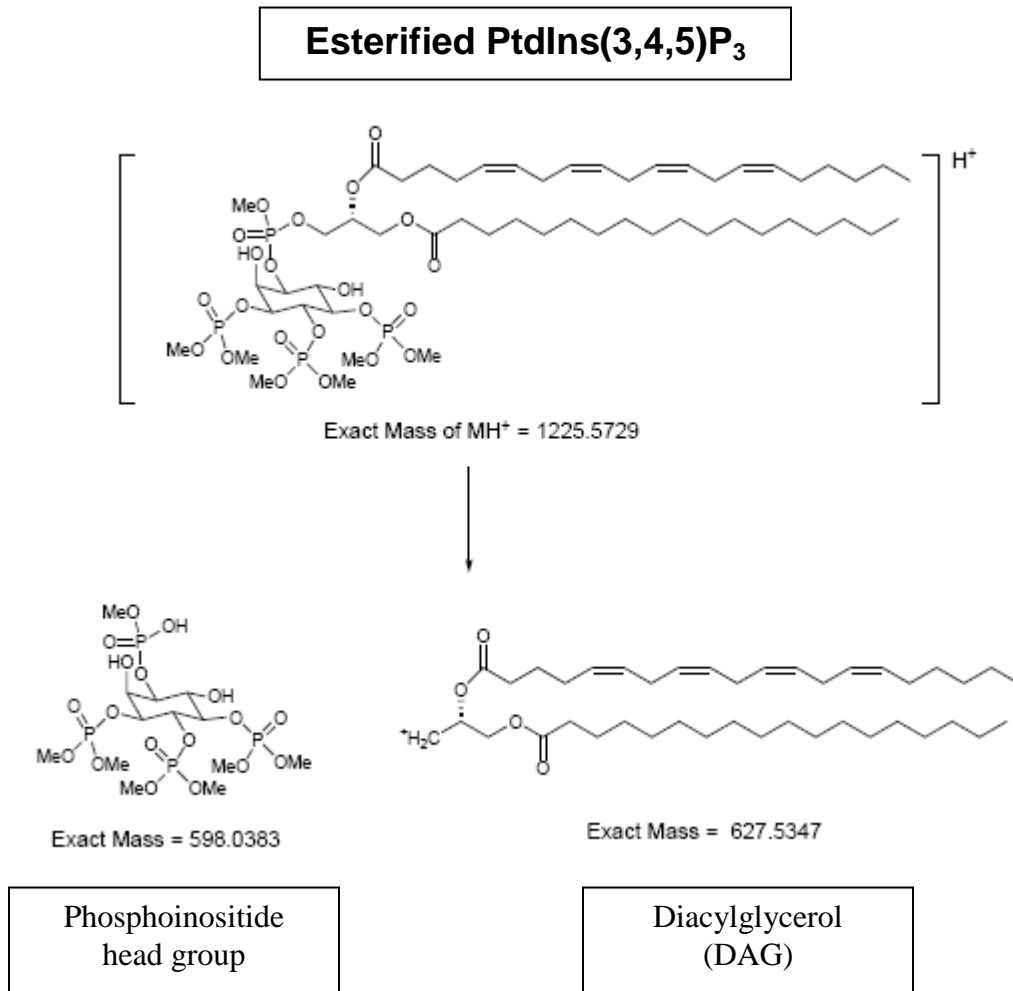


Quantification of PtdInsP₃ molecular species in cells and tissues by mass spectrometry

Jonathan Clark, Karen E Anderson, Veronique Juvin, Trevor S Smith, Fredrik Karpe, Michael J O Wakelam, Len R Stephens & Phillip T Hawkins

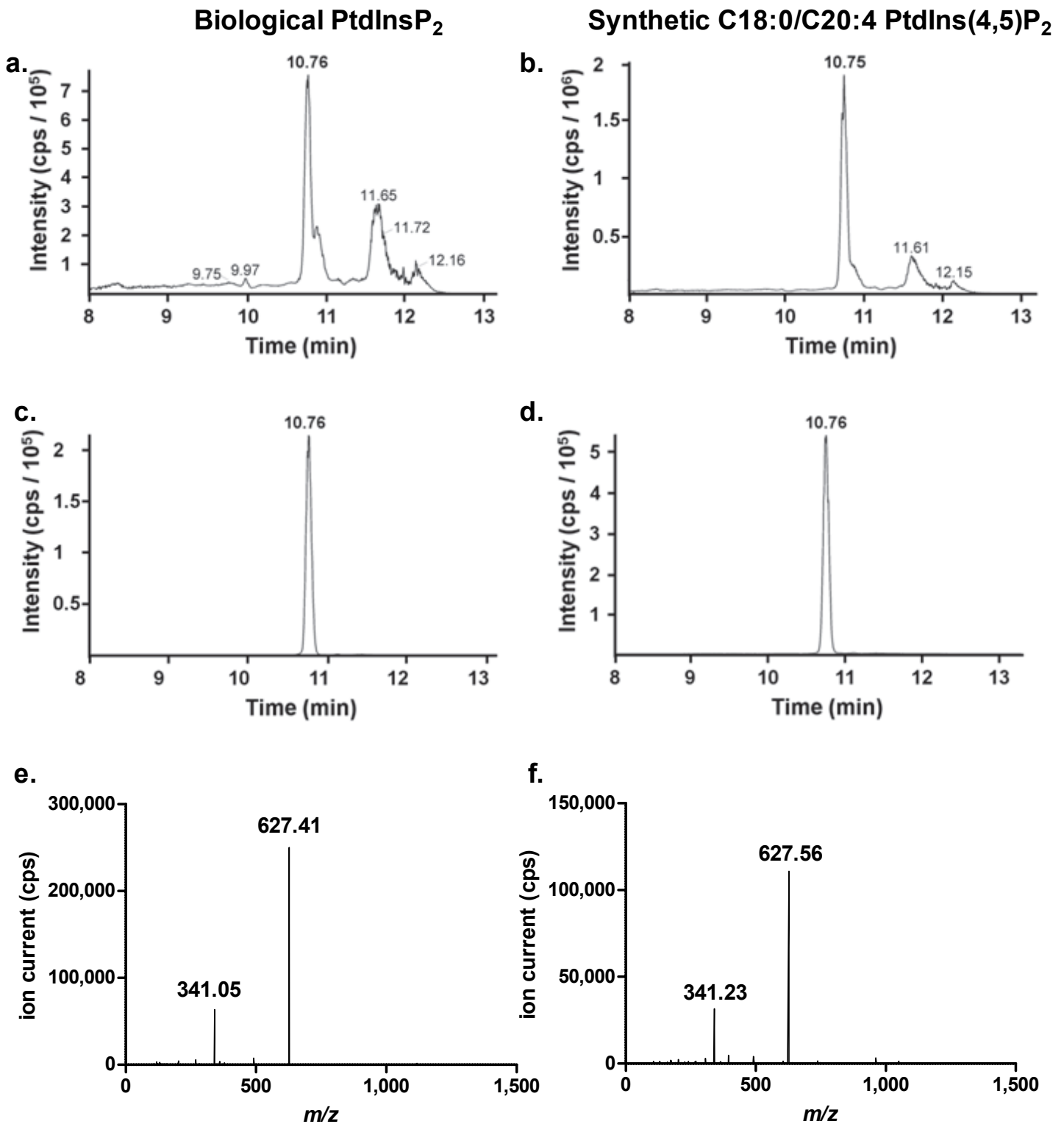
Supplementary Figure 1	Masses and structures of methylated C18:0/C20:4-PtdIns(3,4,5)P ₃ and its components.
Supplementary Figure 2	Analysis of synthetic C18:0/C20:4-PtdIns(4,5)P ₂ standard and endogenous C18:0/C20:4-PtdInsP ₂ from fMLP-stimulated neutrophils.
Supplementary Figure 3	Analysis of synthetic C18:0/C20:4-PtdIns(3,4,5)P ₃ standard and endogenous C18:0/C20:4-PtdIns(3,4,5)P ₃ from fMLP-stimulated neutrophils.
Supplementary Figure 4	Methylation states of derivatised C18:0/C20:4-PtdIns(3,4,5)P ₃ from fMLP-stimulated neutrophils, and C17:0/C16:0-PtdIns(3,4,5)P ₃ internal standard
Supplementary Figure 5	Validation of the signal-to-noise of C18:0/C20:4-PtdIns(3,4,5)P ₃ in the assay
Supplementary Figure 6	Validation of the assay
Supplementary Figure 7	Validation of the linearity of the assay
Supplementary Figure 8	Comparison of PtdInsP ₃ analysis in control and EGF stimulated wild-type MCF10a cells by mass spectrometry and ³ H-inositol labelling
Supplementary Figure 9	Detection and quantification of C18:0/C20:4 PtdInsP ₂ in mouse liver in response to insulin, and in human adipose tissue before and after oral ingestion of glucose.
Supplementary Figure 10	Detection of PKB phosphorylation in mouse liver in response to insulin, and in human adipose tissue before and after oral ingestion of glucose.
Supplementary Table 1	Structures of DAG fatty acid species of detected phospholipids and masses of relevant parent species.
Supplementary Table 2	Structure and Masses of methylation states of C18:0/C20:4- PtdInsP ₂ , PtdIns(3,4,5)P ₃ and PtdSer.
Supplementary Data 1	Quattro Ultima mass spectrometer parameters
Supplementary Data 2	QTRAP 4000 mass spectrometer parameters

Supplementary Figure 1: Masses and structures of methylated C18:0/C20:4-PtdIns(3,4,5)P₃ and its components.



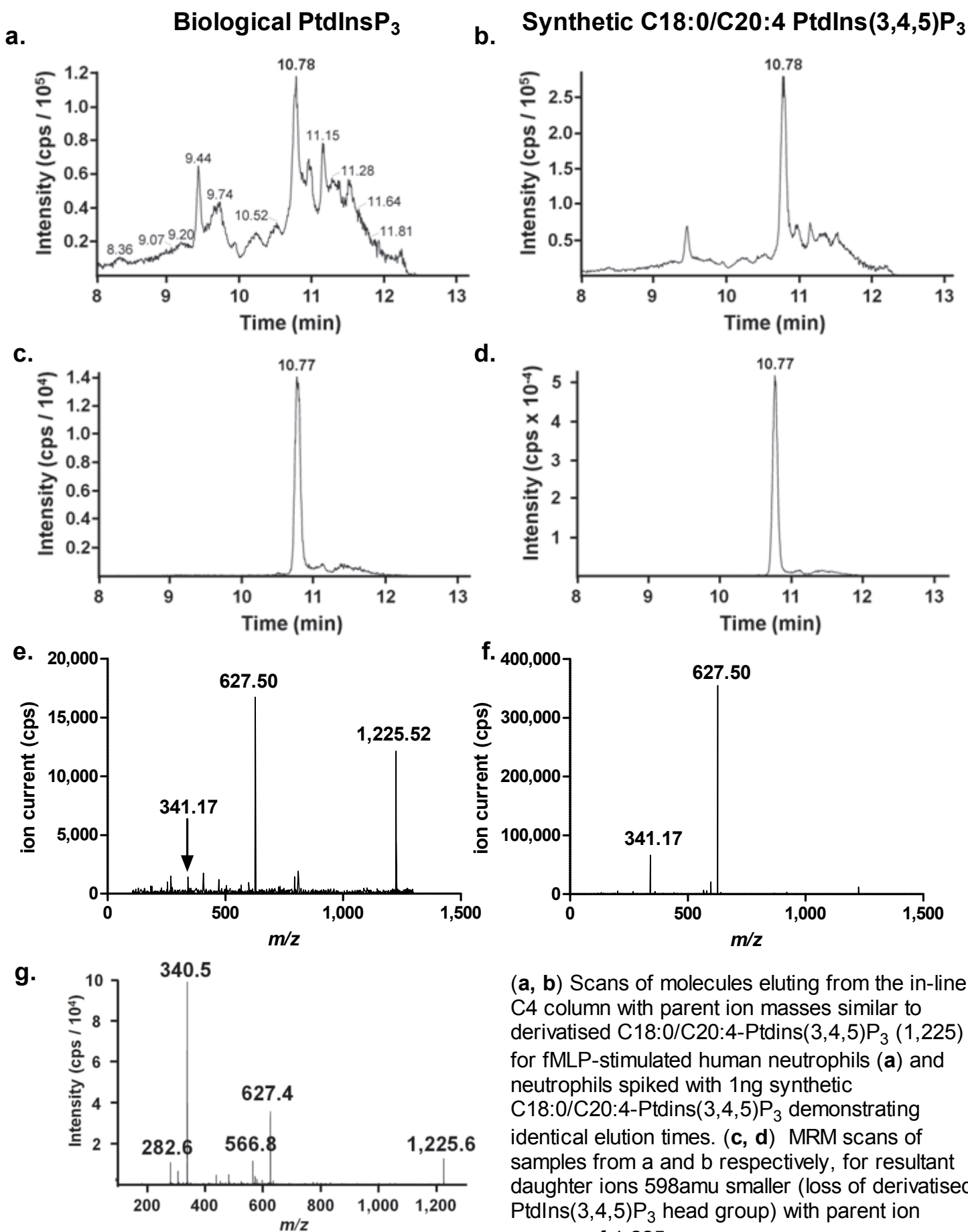
Structural diagram and exact mass of methylated C18:0/C20:4-PtdIns(3,4,5)P₃, including the complete molecule, and resultant cleavage between the phosphoinositide head group and the glycerol unit, yielding a neutral loss of a fragment corresponding to the derivatised inositol phosphate head group and charged fragment corresponding to the diacylglycerol (DAG).

Supplementary Figure 2: Analysis of synthetic C18:0/C20:4-PtdIns(4,5)P₂ standard and endogenous C18:0/C20:4-PtdInsP₂ from fMLP-stimulated neutrophils.



(a, b) Scans of molecules eluting from the in-line C4 column with parent ion masses similar to derivatised C18:0/C20:4-PtdInsP₂ (1,117) for fMLP-stimulated human neutrophils (a) and neutrophils spiked with 10 ng synthetic C18:0/C20:4-PtdIns(4,5)P₂ demonstrating identical elution times. (c, d) MRM scans of samples from a and b respectively, for resultant daughter ions 490 amu smaller (loss of derivatised PtdInsP₂ head group) with parent ion masses of 1,117. (e) Fragmentation profile, from MS2 scan, from fMLP-stimulated neutrophils, of parent ion of mass 1,117 (i.e. possible C18:0/C20:4-PtdInsP₂ species) showing production of daughters identical to those produced in fragmentation profiles of synthetic C18:0/C20:4-PtdIns(4,5)P₂ standard (f). Data (e, f), and those in Supplementary Fig 3e and f, and Supplementary Figs. 5-8, were collected with a Quattro Ultima mass spectrometer, while all other data (a-d) and those in Supplementary Figs. 3a-d,g, 4 and 9 were produced using a QTRAP 4000 mass spectrometer. All are representative traces.

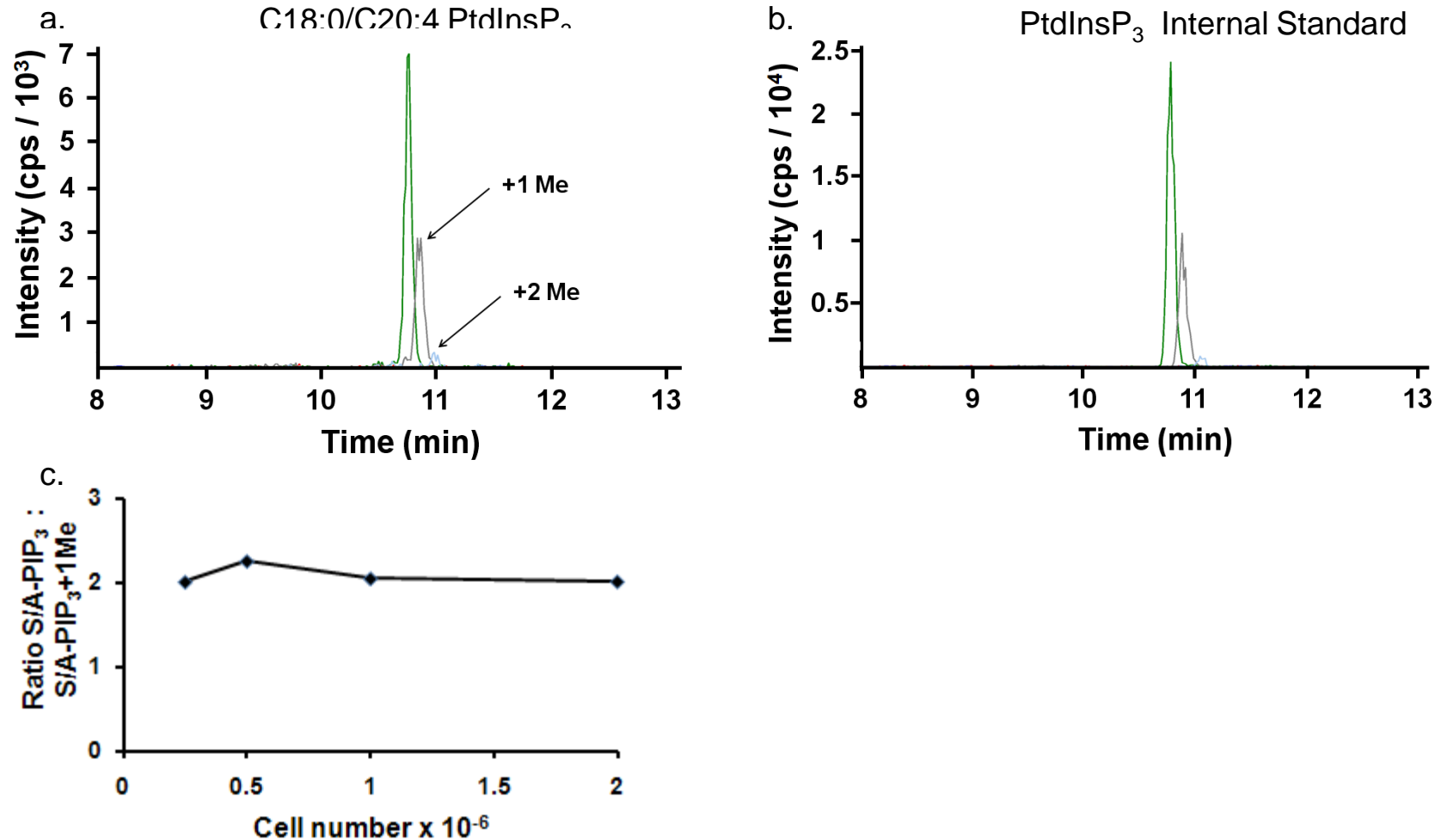
Supplementary Figure 3: Analysis of synthetic C18:0/C20:4-PtdInsP₃ standard and endogenous C18:0/C20:4-PtdInsP₃ from fMLP-stimulated neutrophils.



(a, b) Scans of molecules eluting from the in-line C4 column with parent ion masses similar to derivatised C18:0/C20:4-Ptdins(3,4,5)P₃ (1,225) for fMLP-stimulated human neutrophils (a) and neutrophils spiked with 1ng synthetic C18:0/C20:4-Ptdins(3,4,5)P₃ demonstrating identical elution times. (c, d) MRM scans of samples from a and b respectively, for resultant daughter ions 598amu smaller (loss of derivatised PtdIns(3,4,5)P₃ head group) with parent ion masses of 1,225.

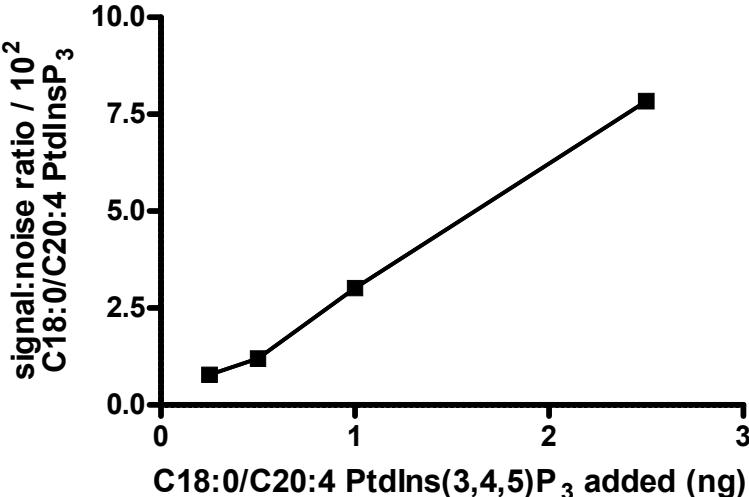
(e-g) (e) Fragmentation profile, from MS² scan, from fMLP-stimulated neutrophils, of parent ion of mass 1,225 (i.e. possible C18:0/C20:4-PtdIns(3,4,5)P₃ species) showing they produce daughters identical those produced in fragmentation profiles of synthetic C18:0/C20:4-PtdIns(3,4,5)P₃ standard (f). (g) Fragmentation profile from an EPI scan of material like that in (e).

Supplementary Figure 4 : Methylation states of derivatised C18:0/C20:4-PtdIns(3,4,5)P₃ from fMLP-stimulated neutrophils, and C17:0/C16:0-PtdIns(3,4,5)P₃ internal standard.



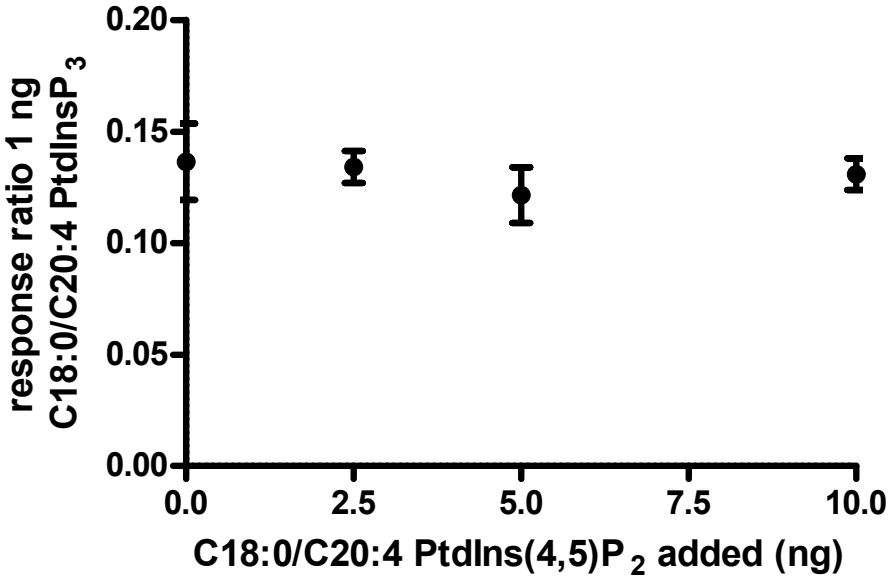
Overlay of MRM scans of derivatised endogenous C18:0/C20:4-PtdIns(3,4,5)P₃ in an extract of fMLP-stimulated human neutrophils (a) and 1 ng synthetic C17:0/C16:0-PtdIns(3,4,5)P₃ internal standard spiked into the same neutrophil extract (b), selected for and displaying methylation states of each. No under-methylation was detected. +1 and +2 Me indicate over-methylation on the two free hydroxyls in the inositol ring (2 or 6-positions). No over-methylation was observed on the lipid backbone. Full structures and masses of protonated and methylated phospholipids are described in Supplementary Table 2. (c) Histogram displaying that the degree of over-methylation of C18:0/C20:4-Ptdins(3,4,5)P₃ in fMLP-stimulated neutrophils was not affected by cell number when derivatising samples from 2x10⁵ to 2x10⁶ neutrophils.

Supplementary Figure 5 : Validation of the signal-to-noise of C18:0/C20:4-PtdIns(3,4,5)P₃ in the assay.



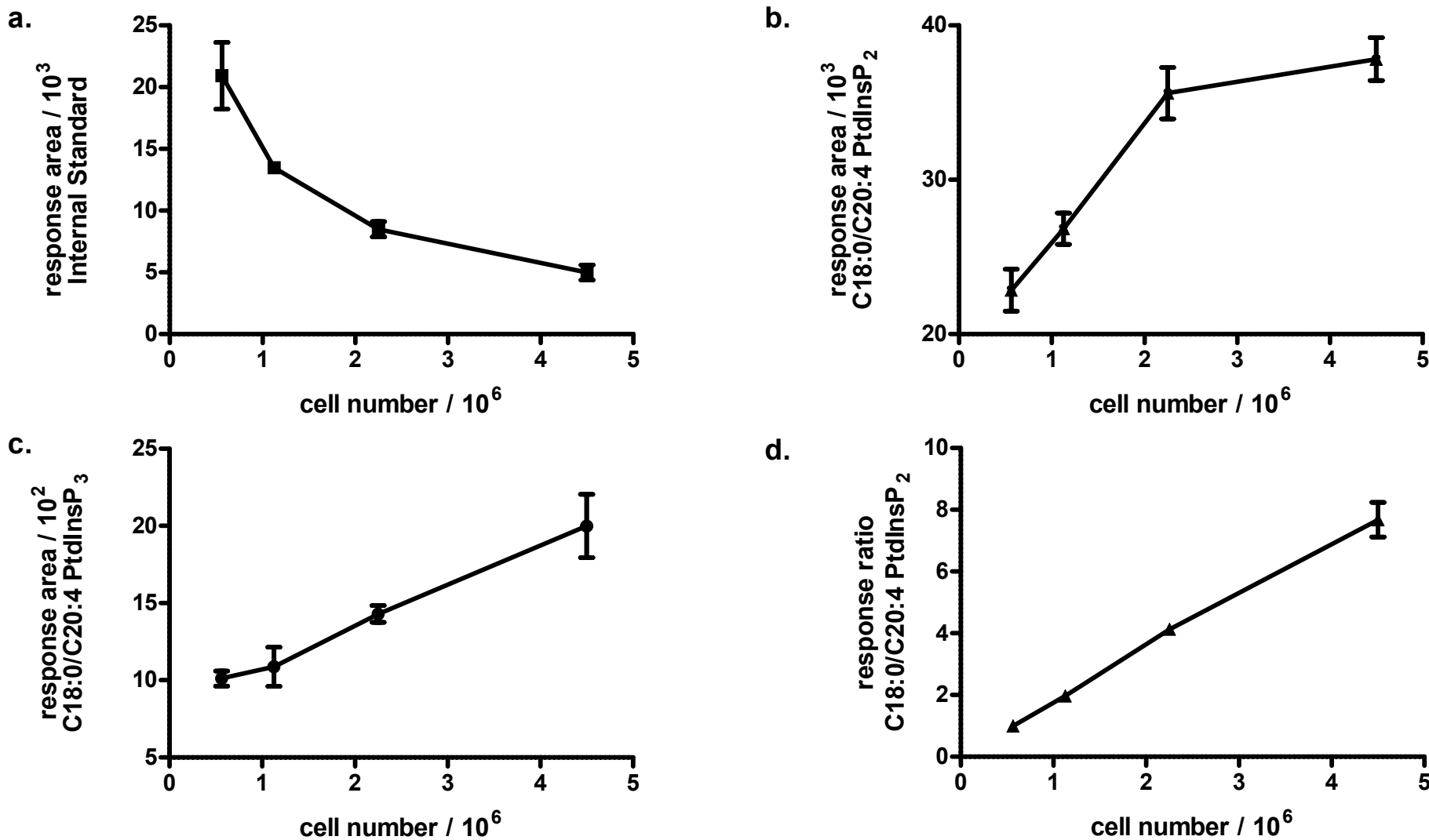
Histogram demonstrating a linear signal-to-noise ratio produced in response to 0.5-2.5 ng C18:0/C20:4-PtdIns(3,4,5)P₃ standard spiked into un-stimulated neutrophil samples.

Supplementary Figure 6 : Validation of the assay.



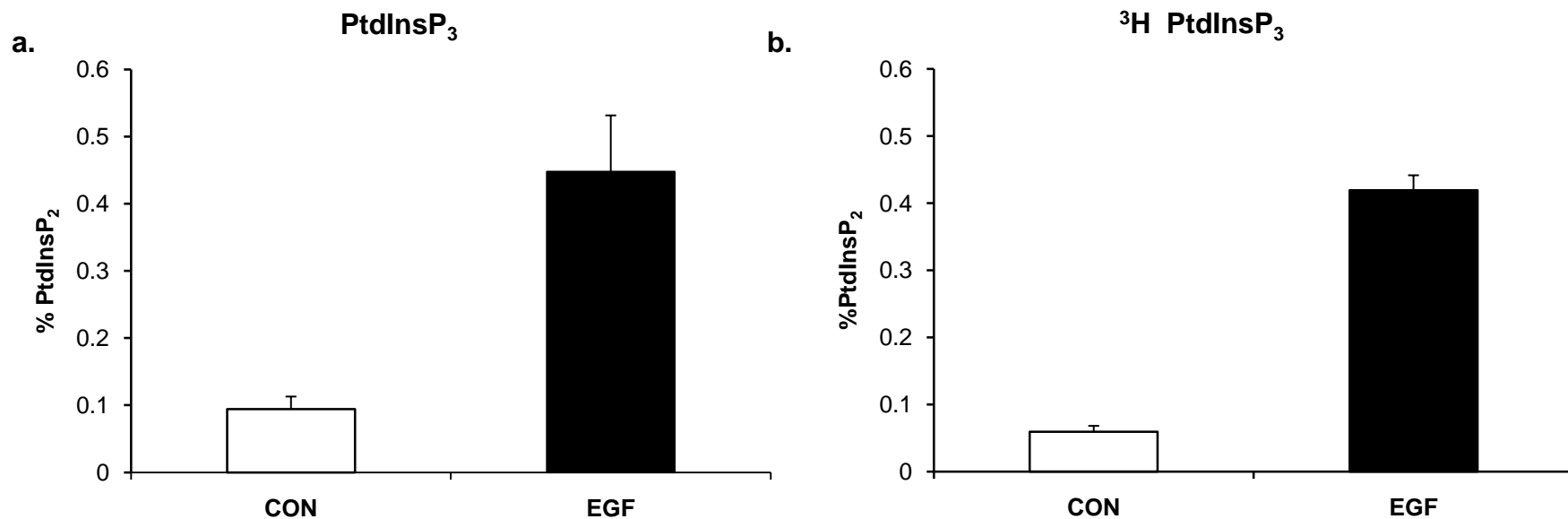
Histograms from human neutrophil samples demonstrating no effect of spiking increasing amounts of C18:0/C20:4 PtdIns(4,5)P₂ standard into un-stimulated neutrophil extracts on quantification of a parallel spike of 1 ng of C18:0/C20:4-PtdIns(3,4,5)P₃ standard.

Supplementary Figure 7: Validation of the linearity of the assay



Histograms from human neutrophil samples demonstrating; **(a)** that recovery of ISD standard is reduced with increasing amounts of neutrophil extract (in separate experiments we used either vehicle-alone or fMLP stimulated neutrophil extracts, however, the data for each were identical and hence were combined for presentation); **(b)** the uncorrected amount of endogenous C18:0/C20:4-PtdInsP₂ that is detected in extracts does not have a linear relationship with cell input (these data were derived from the same experiments that produced the data presented in **(a,c,d** and **Fig 2e**. in the main body of the manuscript)); **(c)** the uncorrected amount of endogenous C18:0/C20:4-PtdIns(3,4,5)P₃ that is detected in extracts does not have a linear relationship with cell input; **(d)** that by using the recovered ISD as a correction factor for recovery of endogenous PtdInsP₂ a linear relationship between cell number and estimated endogenous C18:0/C20:4-PtdInsP₂ was established.

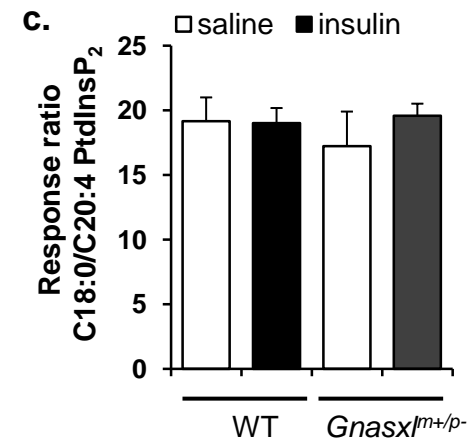
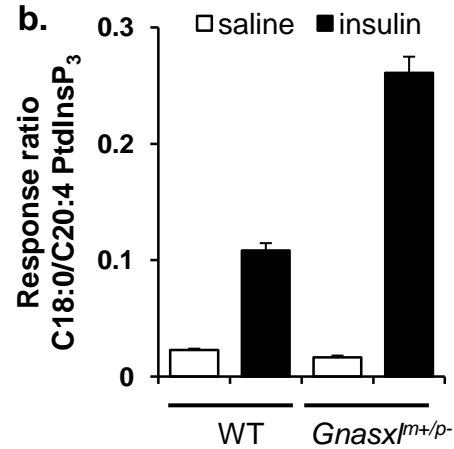
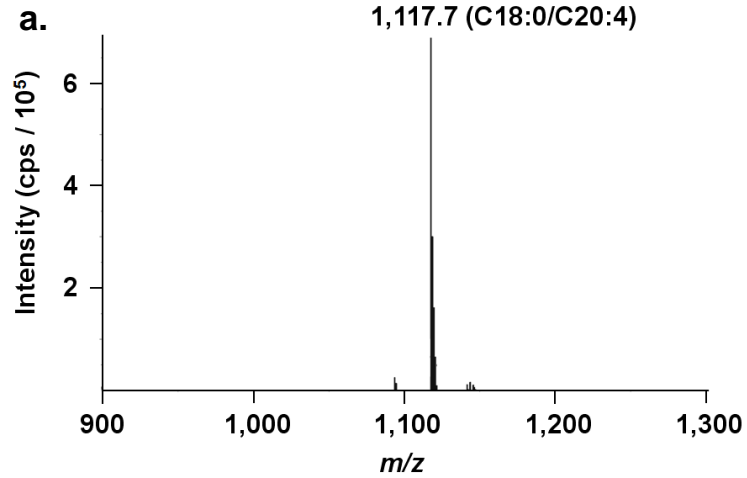
Supplementary Figure 8 : Comparison of PtdInsP₃ analysis in control and EGF-stimulated wild-type MCF10a cells by mass spectrometry and ³H-inositol labelling.



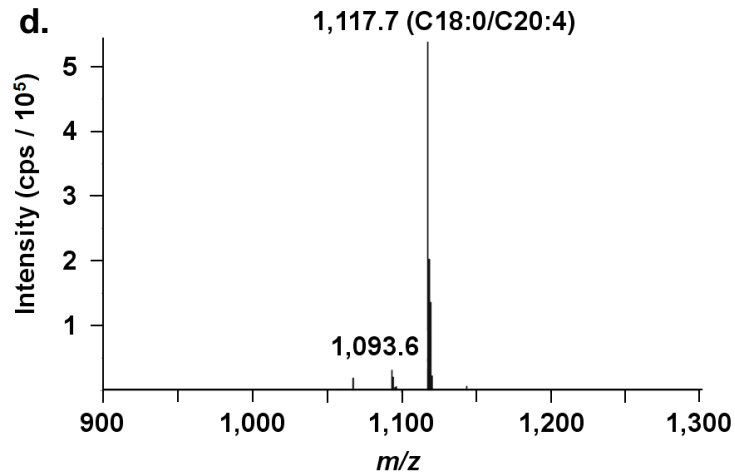
Levels of PtdInsP₃ in wild-type MCF10a cells either starved (CON, 1% dialysed serum in medium containing a final concentration of 4.6 μ M myo-inositol, for 17 hr) or in the presence of EGF (2 min, after starvation) measured by a QTRAP 4000 mass spectrometry (a) or following ³H-inositol labelling (final myo-inositol concentration 4.6 μ M) (b). (a) Data are presented as additive total response ratios of each PtdInsP₃ species (as shown in Figure 4) normalised for cell input *via* the recovered C18:0/C18:1-PtdSer, and to total PtdInsP₂ levels (corrected for the relative efficiency of methylation of PtdInsP₂ compared to PtdIns(3,4,5)P₃) of the samples. (b) Data are presented as average DPM for PtdInsP₃ fractions eluting from HPLC anion-exchange column, normalised to PtdInsP₂ DPM, for each sample.

Supplementary Figure 9: Detection and quantification of C18:0/C20:4-PtdInsP₂ and C18:0/C20:4-PtdInsP₃ in mouse liver in response to insulin, and C18:0/C20:4-PtdInsP₂ in human adipose tissue before and after oral ingestion of glucose.

Mouse Liver



Human Adipose

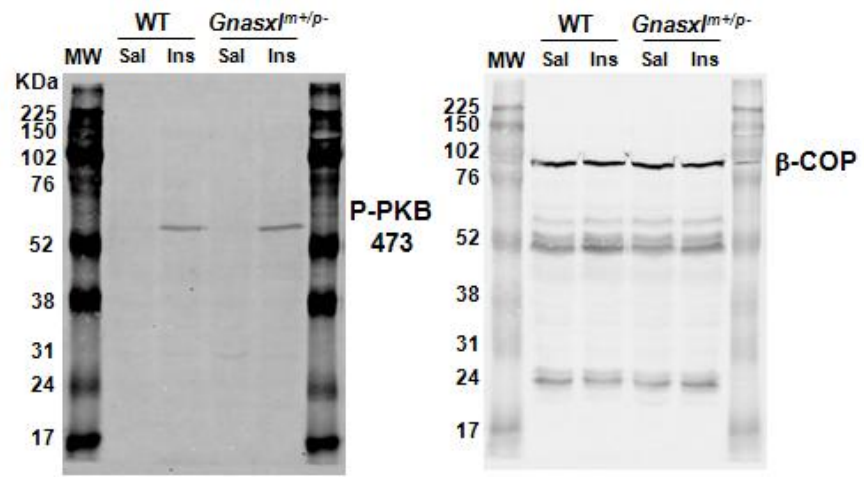


Neutral loss scan of PtdInsP₂ species in insulin-stimulated, wild-type (WT) mouse liver (**a**) and human adipose tissue following oral ingestion of glucose (**d**) showing C18:0/C20:4 is the major fatty acid species. Data quantifying the levels of C18:0/C20:4-PtdInsP₃ (**b**) and C18:0/C20:4-PtdInsP₂ (**c**) from WT mice or those lacking the imprinted isoform of *Gαs*, *Gnasx1^{m+/p-}*, 8 mins after an I.P. injection of insulin or saline are presented as response ratios normalised for cell input *via* the recovered C18:0/C20:4-PtdSer (means ± SEM, n= 4). Data was collected using a QTRAP 4000 mass spectrometer.

Supplementary Figure 10: PKB phosphorylation in mouse liver in response to insulin, and in human adipose tissue before and after oral ingestion of glucose.

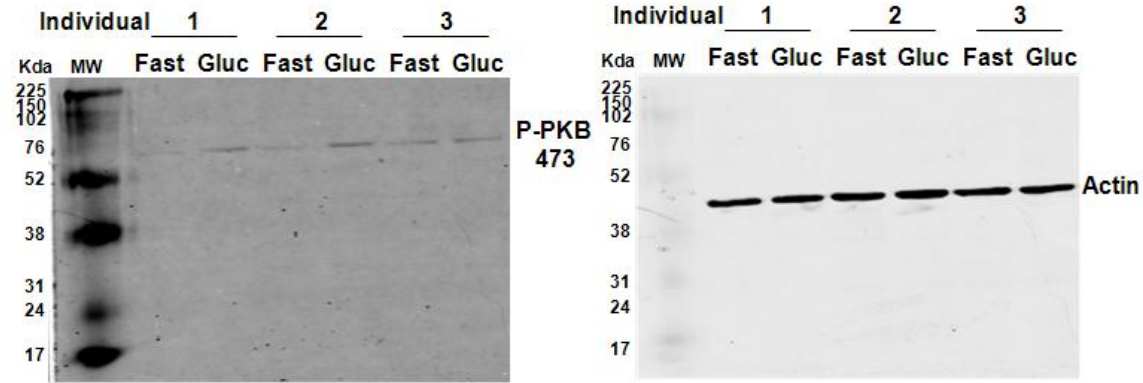
Mouse Liver

a.



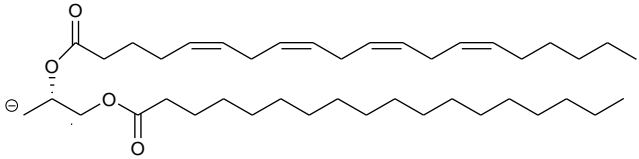
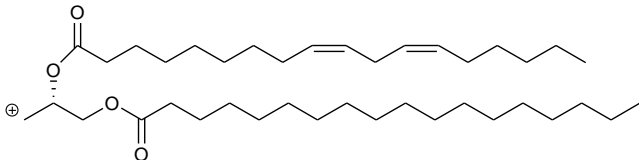
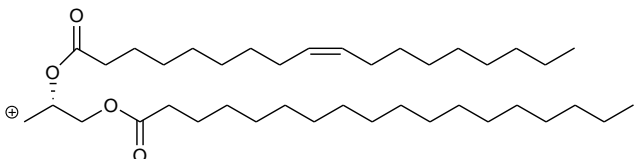
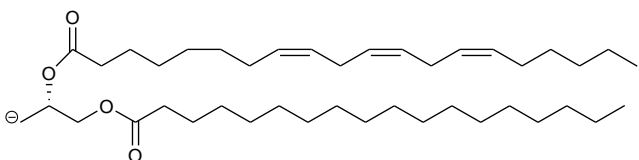
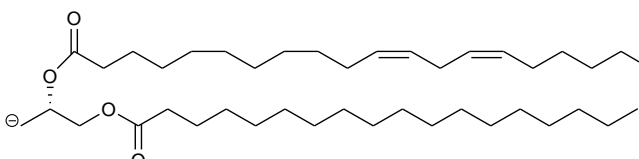
Human Adipose

b.



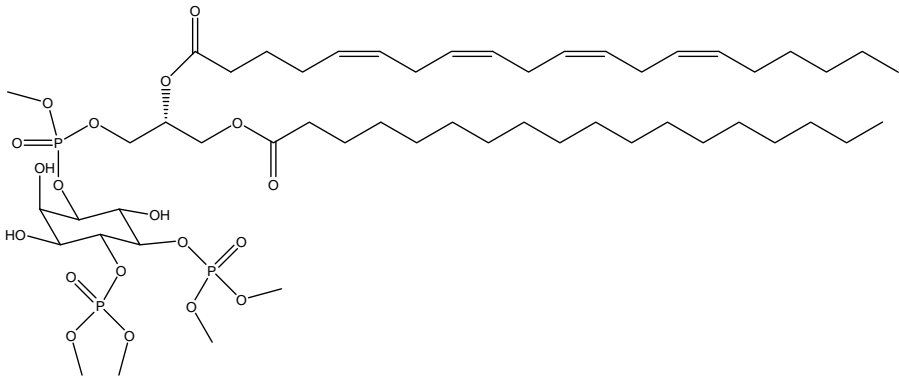
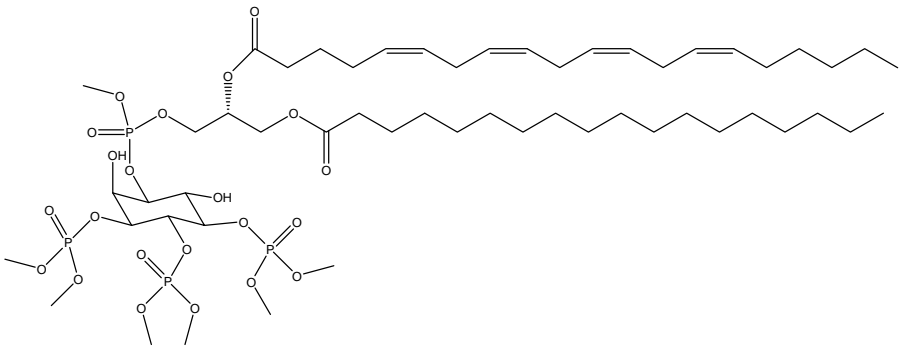
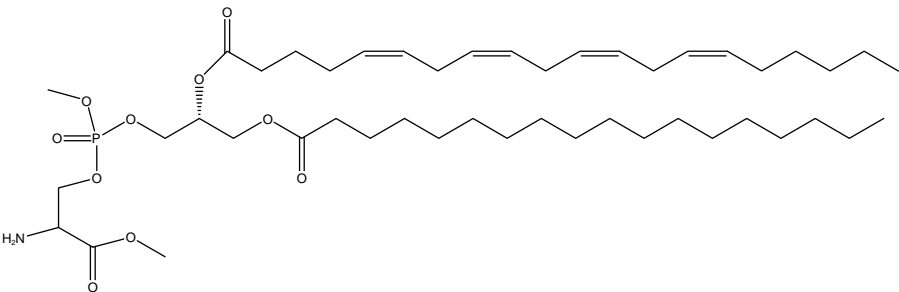
Parallel aliquots, from samples in Supplementary Figure 9, of control and insulin stimulated mouse liver (a), or human adipose tissue pre- and post- oral ingestion of glucose (b), were subjected to quantitative immuno-blotting to reveal the phosphorylation status of S473 in PKB, with parallel immuno-blot for β -COP (a) or actin (b) to use as input material control.

Supplementary Table 1: Structures of DAG fatty acid species of detected phospholipids and masses of relevant parent species.

	DAG+	Parent Species (MH+)		
Neutral loss to add to DAG+ to give parent mass		213.03	490.05	598.00
	MW	PS	PtdInsP ₂	PtdInsP ₃
<p>C18:0 C20:4</p> 	627.54	840.57	1117.59	1225.54
<p>C18:0 C18:2</p> 	603.54	816.57	1093.59	1201.54
<p>C18:0 C18:1</p> 	605.55	818.58	1095.60	1203.55
<p>C18:0 C20:3</p> 	629.59	842.59	1119.59	1227.59
<p>C18:0 C20:2</p> 	631.60	844.60	1121.60	1229.60

Structures of fatty acid species of lipids detected in cell extracts following neutral loss of derivatised head group, and corresponding masses of parent species for PS, PtdInsP₂ and PtdInsP₃. The masses given in the tables are the calculated theoretical exact masses. The difference between these values and those on the Quattro Ultima (Fig. 1) are due to the calibration of the mass spectrometer which was calibrated using the manufacturers best fit routines using a caesium iodide plus sodium iodide mixture. Standards were used to check the deviation of the calibration from theoretical. The newer QTRAP 4000 (Fig. 5) has better mass accuracy after calibration with the manufacturers routines, but the accuracy achieved in neutral loss scanning is in part dependent on the dwell used. A balance is achieved between the mass accuracy and the number of data points when constructing a scanning mass spectrometer experiment. Again standards were tested for a given dwell time to verify any deviation from theoretical. Although with the MRM transitions the mass accuracy is greater, it is also not as relevant because a window +/- 0.5 amu is used to encompass the mass peak.

Supplementary Table 2: Structure and Masses of methylation states of C18:0/C20:4- PtdInsP₂, PtdIns(3,4,5)P₃ and PtdSer.

	Formula	Exact Mass	MH+	MH+Me	MH+2Me
	C ₅₂ H ₉₅ O ₁₉ P ₃	1116.57	1117.57	1131.57	1145.57
	C ₅₄ H ₁₀₀ O ₂₂ P ₄	1224.57	1225.57	1239.57	1253.57
	C ₄₆ H ₈₂ NO ₁₀ P	839.57	840.57		

Full structures of derivatised C18:0/C20:4- PtdInsP₂, PtdIns(3,4,5)P₃ and PtdSer, with formulas, and masses of protonated and over-methylated forms of the phospholipids. The PtdIns(3,5)P₂ and PtdIns(3,4)P₂ have the same mass as the PtdIns(4,5)P₂.

Supplementary Data 1: Quattro Ultima mass spectrometer parameters:

Capillary voltage 3.0 kV
Cone voltage 100 V
Hex 1 0.1 V
Aperture 0.2 V
Hex 2 0.4 V
Source temperature 100 °C
Desolvation Temperature 300 °C
Cone Gas Flow 85 L Hr⁻¹
Desolvation Gas Flow 583 L Hr⁻¹
LM1 Resolution 14
HM 1 Resolution 14
Ion Energy 1 1.2
Entrance 18
Collision 30
Exit 18
LM2 Resolution 14
HM 2 Resolution 14
Ion Energy 2 1.5
Multiplier 638 V
CID Argon 5 psi
Polarity Positive

Waters 2795 HPLC

Solvent A: Water, 0.1% trifluoroacetic acid (TFA)

Solvent B: Acetonitrile, 10% water, 0.1% TFA

Column: Phenomenex 1 mm x 50 mm C4 Jupiter column

Gradient:

Time (min)	A%	B%	Flow (ml min⁻¹)	Curve
0	25	75	0.1	1
5	25	75	0.1	6
10	0	100	0.1	6
15	0	100	0.1	6
20	0	100	0.1	6
25	25	75	0.1	6
30	25	75	0.1	6

MRM transitions:

<u>Q1 Mass (Da)</u>	<u>Q3 Mass (Da)</u>	<u>Dwell(s)</u>	
1,163.12	565.46	1	C17:0 C16:0 PtdIns(3,4,5)P ₃ Internal Standard
1,224.96	627.30	1	C18:0 C20:4 PtdInsP ₃
1,117.05	627.30	1	C18:0 C20:4 PtdInsP ₂
1,202.90	605.35	1	C18:0 C18:1 PtdInsP ₃
1,095.00	605.35	1	C18:0 C18:1 PtdInsP ₂

Supplementary Data 2: QTRAP 4000 mass spectrometer parameters:

CUR: 20
IS: 4500
TEM: 300
GS1: 18
GS2: 20
ihe: ON
CAD: Medium
DP 100
EP 10
CE 35
CXP 10

Acquity HPLC:

Solvent A: Water 0.1% Formic Acid

Solvent B: Acetonitrile 0.1% Formic acid.

Column: Waters Acquity UPLC BEH 300 C4 1.7 μ m, 1.0 x 100 mm column

Gradient:

Time (min)	Flow Rate	%A	%B	Curve
0	0.1	55	45	
5	0.1	55	45	6
10	0.1	0	100	6
15	0.1	0	100	6
16	0.1	55	45	6
20	0.1	55	45	

MRM transitions:

Polarity: Positive
Ion Source: Turbo Spray
Resolution Q1: Unit
Resolution Q3: Low

<u>Q1 Mass (Da)</u>	<u>Q3 Mass (Da)</u>	<u>Dwell(msec)</u>	
1163.60	565.60	50.00	C17:0 C16:0 PtdIns(3,4,5)P ₃ Internal Standard
1225.57	627.60	50.00	C18:0 C20:4 PtdInsP ₃
1117.22	627.60	50.00	C18:0 C20:4 PtdInsP ₂
1227.59	629.60	50.00	C18:0 C20:3 PtdInsP ₃
1119.59	629.60	50.00	C18:0 C20:3 PtdInsP ₂
1201.57	603.53	50.00	C18:0 C18:2 PtdInsP ₃
1093.58	603.53	50.00	C18:0 C18:2 PtdInsP ₂
1203.59	605.60	50.00	C18:0 C18:1 PtdInsP ₃
1095.59	605.60	50.00	C18:0 C18:1 PtdInsP ₂
1229.60	631.56	50.00	C18:0 C20:2 PtdInsP ₃
1121.60	631.56	50.00	C18:0 C20:2 PtdInsP ₂
818.58	605.60	50.00	C18:0 C18:1 GPtdSer

901.57	627.60	50.00	C18:0 C20:4 PtdIns
1009.57	627.60	50.00	C18:0 C20:4 PtdInsP
877.57	603.53	50.00	C18:0 C18:2 PtdInsP
985.57	603.53	50.00	C18:0 C18:2 PtdIns
879.59	605.60	50.00	C18:0 C18:1 PtdInsP
987.59	605.60	50.00	C18:0 C18:1 PtdIns
905.60	631.56	50.00	C18:0 C20:2 PtdInsP
1013.60	631.56	50.00	C18:0 C20:2 PtdIns
840.57	627.60	50.00	C18:0 C20:4 PtdSer
1011.59	629.60	50.00	C18:0 C20:3 PtdInsP
903.59	629.60	50.00	C18:0 C20:3 PtdIns